Journal of Engineering and Applied Sciences 13 (Special Issue 7): 5605-5611, 2018
ISSN: 1816-949X

Design and Development of Transcatheter Aortic Valve Repair (TAVR) Nitinol Stent

[1]K. Kalaiselvam, [1]K. Rajkumar, [2]G. Joseph and [1, 3]M. Thanikachalam
[1]Research and Development Programme, Agada Medical Technologies Private Limited, Chennai, India
[2]Department of Cardiology, Christian Medical College, Vellore, India
[3]Department of Cardiology, Tufts University, Massachusetts, United States

Abstract: Aim of the project is to design a TAVR stent for percutaneous treatment of aortic stenosis, without the need for open heart surgery. Nitinol stent with two interlocked 26 mm diameter zigzag rings was modeled and analyzed in ANSYS 12.0. The various design parameters included the number (n = 10-18) and height (h = 3-6 mm) of struts and the thickness (t = 0.25-0.5 mm) and stiffness (e = 26364M-50000 MPa) of the ring. The FEA was done by altering design parameters to arrive at an optimal crimp profile and radial force for a stent deployed in a 21 mm annulus. Subsequently, buckling and fatigue analysis were performed. Finally, a nitinol stent was prototyped and compression tests were performed to assess the radial force. Among the various parameters, increasing the ring thickness (0.25-0.5 mm) resulted in maximum increase in hoop forces (3.84-10.56 N). At the same time, the minimum crimp profile increased marginally (5.74-6.66 mm). There were minimal changes to hoop forces with changes with number of struts (3.84-4.24 N) or the stiffness of the wire (3.84-4.16). The final optimized design had a crimp profile of 3 mm and a radial force of 16N which was confirmed to be 14 N by compression test. The buckling load was 2.7 N while the fatigue analysis showed durability at 400 million life cycles. Based on FEA, a TAVR stent of acceptable profile, radial force and durability was designed. Further bench testing will validate the design.

Key words: Aortic stenosis, FEA, Nitinol, prototype, stent, buckling, prototyped

INTRODUCTION

Degenerative aortic valve stenosis is the most common valvular disease, affecting about 3% of individuals over the age of 65 (Otto *et al*., 1999) and more than 10% of adults over the age of 75 (Lindroos *et al*., 1993). Open-heart surgical replacement is the standard treatment of aortic valvular disease (Passik *et al*., 1987) but may not be tolerated by a segment of the elderly patient population due to age-related co-morbidities (Roques *et al*., 1999; Kvidal *et al*., 2000; Edwards and Taylor, 2003). Consequently, about one-third of elderly patients with symptomatic aortic stenosis is deemed high risk and are declined surgery (Iung *et al*., 2003). Transcatheter Aortic Valve Replacement (TAVR) is a potential treatment solution in this high-risk patient population.

TAVR includes a bioprosthetic valve loaded inside a stent which is inserted percutaneously through the peripheral vessels using a catheter and implanted at the annulus of the aortic valve. There are few TAVR devices under clinical trial (Zajarias and Cribier, 2009; Zahn *et al*., 2010; Lefevre *et al*., 2010; Moat *et al*., 2011). Clinical experiences with these TAVR devices have confirmed its promise while simultaneously highlighted the limitations of a technique still in development (Ghanbari *et al*., 2008). The critical mechanical properties of the TAVR device are the radial force, crimping ability, buckling load and the durability (Jilaihawi *et al*., 2009).

The self-expanding valve-stent frame made of super elastic nitinol, a nickel-titanium alloy, depends on the radial self-expansion mechanism once deployed. In the current study, we aim to understand the material, design and prototype determinants of the nitinol valve-stent.

We also attempt to optimize the minimum crimp diameter of the stent to facilitate the loading of the stent into a low-profile delivery system and ensure deployablity of the TAVR device through the femoral artery.

MATERIALS AND METHODS

Device description: In this study, the TAVR stent was modeled as two interlocking nitinol rings at the aortic annular region with stabilizers that extend to the SinoTubular Junction (STJ). The rings in the annular region play a vital role the radial force exerted by these rings on the annulus and Left Ventricular Outflow Tract (LVOT) help the device stay in place, avoiding device migration and paravalvular leak. The rings were made of Nitinol. Nitinol's shape memory properties,

Corresponding Author: K. Kalaiselvam, Research and Development Programme, Agada Medical Technologies Private Limited, Chennai, India

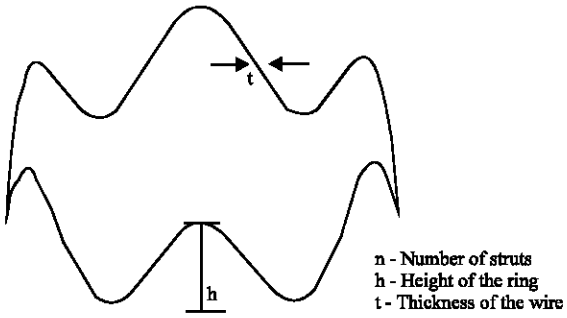

Fig. 1: Geometric model of stent ring

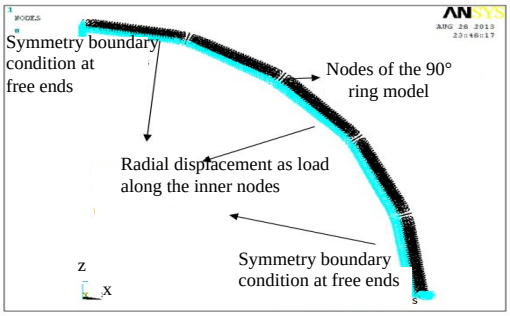

Fig. 2: Loads and boundary condition

biocompatibility, fatigue resistance, strength and MRI compatibility makes it widely used in medical devices (Booher and Eagle, 2011). The material properties and the dimensions of the nitinol ring are important factors that will decide the profile and mechanical properties of the device.

Stent geometry for FEA simulation: The parameters used to define the nitinol stent geometry included the number of struts (n), the height of the ring (h), the thickness of the nitinol wire (t) and the stiffness of the nitinol wire (e). Rings were modeled with various combinations of above parameters and were subjected to FEA (Fig. 1). Maintaining the shape of the ring and its diameter (26 mm) as constants, the parameters (n, h, t and e) were changed. The parametric values were n = 10, 12, 14, 16 and 18; h = 3, 4, 5, 6 and 7.5 mm t = 0.25, 0.3, 0.35, 0.4, 0.45 and 0.5 mm and stiffness of the nitinol wire (e) = 26364 and 50000 MPa.

Finite element model: ANSYS Multi Physics (V. 12.0) Software was employed to perform the finite element analysis. The stent was meshed with 8 noded SOLID185 elements. The appropriate material properties of nitinol, viz. elastic modulus and stress values that defined the transformation curve and the maximum superelastic strains were defined (Cunningham *et al*., 2004). Meshing was done such that number of elements at the bends was greater than those in other areas because the bends were expected to experience larger strain than the surrounding regions.

Crimping analysis: The minimum crimp profile helps in easy deployability through femoral artery. The symmetrical nature of the design required only the 90° segment of the stent ring to be modeled and analyzed. In the FEA Model, the work plane was changed to cylindrical co-ordinate system in which the Y coordinate was assumed to be in the axial direction and X and Z in the perpendicular radial directions. In the axial direction, the displacements at the bottom of the model were constrained and freely allowed at the top. The innermost nodes of the struts throughout the circular region were selected and the radial inward displacement of 11.5 mm was applied. All the nodes were moved to the new co-ordinate system to ensure the radial displacement of the ring. The first load step was created (Fig. 2).

Determination of radial force by FEA: Keeping the boundary condition constant, once the device was crimped, the displacement was applied along the same nodes in the opposite direction to simulate the deployment of the stent at the annulus. The second load step was created. The static non linear analysis with two load steps was solved using sparse solver. The stent was deployed in annulus diameters varying from 21-26 mm. Nitinol possesses super elastic properties and therefore, the device would exert a force when it is deployed in a annulus which is narrower than its original diameter of the stent (26 mm). This resultant force that is determined quantifies the radial force of the device.

Determination of buckling load: After deployment when blood enters the device, axial load is exerted on it which could cause the device to buckle. Analysis was conducted in a stent model with optimized design parameters based on radial force and crimping analysis. The stent model was constrained in all degrees of freedom at the bottom and axial load of 230 mmHg (0.03606 N) was applied on the top of the device. The analysis was approached as Eigen buckling and it was solved with block lanczos mode extraction method.

Determination of fatigue load: For a 10 years lifetime, the stent is expected to experience 400 million cycles of alternating forces arising from pulsating blood pressure. Analysis of the device was performed by doing the

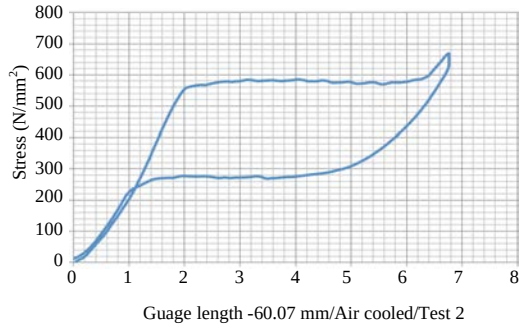

Fig. 3: Stress-strain curve for 0.5 mm diameter wire

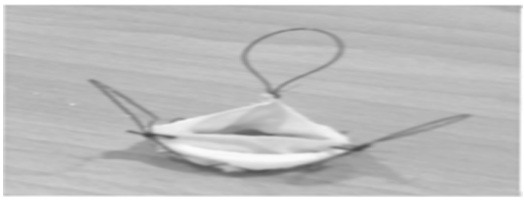

Fig. 4: TAVR stent with tissue valve

transient analysis with the load curve of minimum and the maximum blood pressure considered for loading; 0.0067N/mm^2 (50 mm Hg) and 0.019 N/mm^2 (150) mm Hg) respectively. Subsequent to the transient analysis, fatigue analysis was initiated with specific locations (scaffold, commissures and hook) and event (400 million life cycle for each location). Stress-Strain curve (Fig. 3) for shape set nitinol was given as input for its material property. Analysis was solved for different annulus diameters: 20-23 mm.

Prototype and testing for radial force: Based on the final design as per FEA, the stents were prototyped as per specified manufacturing process for shape setting the nitinol wires. Subsequently, stents were interlocked and welded and the bovine tissue valve was sutured to the inside of the composite stent to create a stent-valve device (Fig. 4).

The device was tested for radial force by the tensile machine (ADMET Mtest quttro Norwood, MA). It was placed between two flat mandrels and pressure was applied on the mandrel to compress the device from 26 mm diameter to 21 mm diameter. Radial force was measured for the device at 21 mm diameter.

RESULTS AND DISCUSSION

Radial force and crimping analysis: Increase in ring thickness from 0.25-0.5 mm resulted in rapid increase of radial force from 3.84-10.86 N at 21 mm deployment diameter. At 0.5 mm ring thickness, progressive decrease in the number of struts from 18-10 resulted in the radial force increase from 9-16 N. Another parameter that greatly influenced the radial force was the height of the ring. The decrease in the height of the ring from 6-3 mm caused an increase in radial force increased from 8-18 N (Fig. 5: Panel A).

The change in the stiffness of the material resulted in negligible change in the radial force. The increase in the thickness of the nitinol ring from 0.25-0.5 mm resulted in an increase in the minimum crimp diameter from 5-6.6 mm. The decrease in the number of struts from 18-10 caused the crimp diameter of the ring to decrease from 7.6- 4.8 mm, while the decrease in the height of the ring from 6-3 mm resulted in an increase in the minimum crimp diameter of the ring from 4.8-7.3 mm (Fig. 5: Panel B).

Based on the above analysis, it is seen that the deployment diameter, thickness and height of the rings are major determinants of radial force. The increase in thickness and height of the rings increases the minimum crimp diameter. At given ring thickness and height, the radial force and crimp diameter can further be optimized by manipulating the number of struts. Thus, an optimal combination of thickness, height, number of struts of nitinol rings and over sizing the stent could result in adequate radial force and desired crimp profile.

Based on multiple analysis, the stent parameters were optimized to yield a crimp profile of 3 mm with a radial force of 16 N when deployed in a 21 mm annulus. The final optimized stent design parameters were n = 10; h = 50 mm; Wire thickness (t) = 0.5 mm; Diameter = 26 mm and stiffness (e) = 26364 MPa.

Buckling analysis: Buckling is experienced only along the long unsupported region of the stabilizers. The stabilizers function to orient the device inside the vessel, hence, minimal buckling this region of the device is acceptable and can be ignored (Fig. 6). Device is initiated with the maximum load of 230 mmHg (0.03606N). The device started to buckle at the factor of 0.7, i.e., the device can withstand 3.5 N force.

Fatigue analysis: The device was tested for 400 million life cycles. Durability of the device observed in the analysis was satisfactory. The stress and strain values of beam elements were obtained from the element table e-table (ANSYS Software). E-table tabulated all the stress and strain values representing at specified locations in the cross section of the beam elements. From the strain table, the strain amplitude was calculated for each element. The maximum strain amplitude was obtained from the tables (Fig. 7)

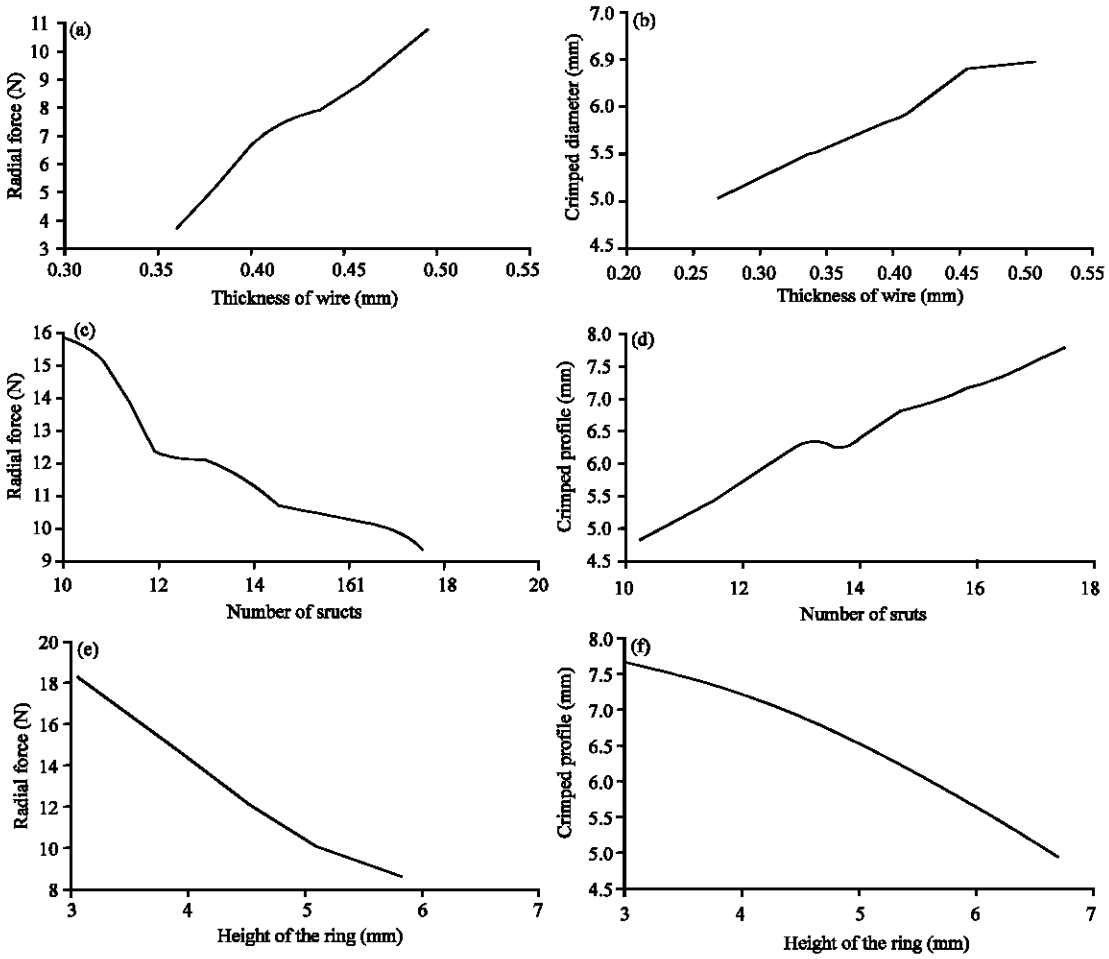

Fig. 5: Panel A: Radial force vs. various design parameters; Panel B: Crimp profile vs. various design parameters

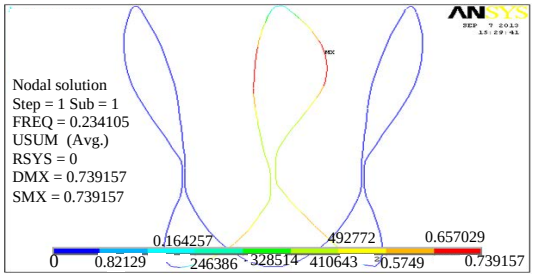

Fig. 6: Buckling results-displacement plot

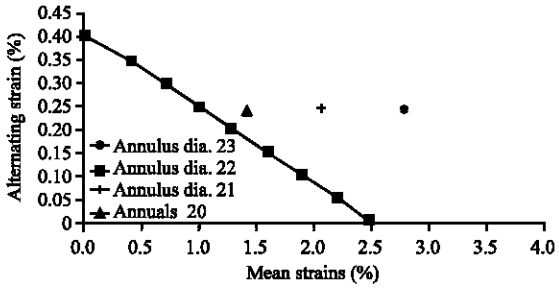

Fig. 7: Fatigue analysis-results haig plot

From the nitinol reference SN curve (Fig. 3), the haigh diagram (Fig. 8) was drawn with the calculated mean strain and strain amplitude to show whether the device withstands 400 million cycles. In the plot the alternating strain value for diameter 23 mm is very close to the SN curve.

Based on the haigh plot (Fig. 8 and 9) it was concluded that the device can with stand 400 million life cycles when deployed in the annulus diameter of 23 mm.

Radial force by compression testing: Based on the compression testing, the radial force was 14 N at 22 mm diameter (Fig. 10), almost similar to 16 N derived from FEA analysis. It is showing that the device has enough radial force below 22 mm diameter. The below plot is drawn by the taking the value from the compression testing machine which shows the radial force (N) vs stent diameter (Fig. 9).

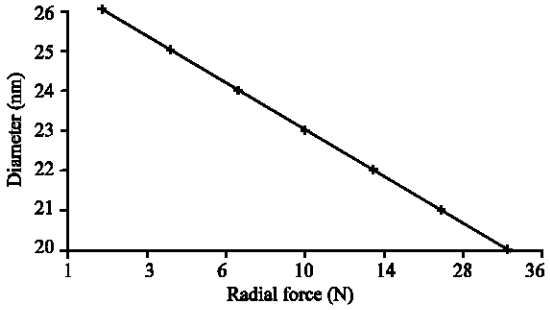

Fig. 8: Radial force vs. diameter curve by compression testing

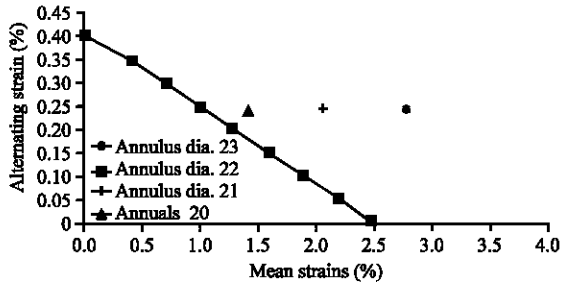

Fig. 9: Fatigue analysis-results haig plot

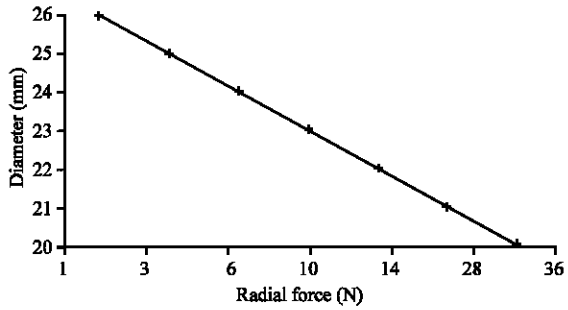

Fig. 10: Radial force vs. Diameter curve by compression testing

Fatigue analysis: The device was tested for 400 million life cycles. Durability of the device observed in the analysis was satisfactory. The stress and strain values of beam elements were obtained from the element table e-table (ANSYS Software). E-table tabulated all the stress and strain values representing at specified locations in the cross section of the beam elements. From the strain table, the strain amplitude was calculated for each element. The maximum strain amplitude was obtained from the tables (Table 1 and 2).

From the Nitinol reference SN curve (Fig. 3), the haigh diagram (Fig. 8) was drawn with the calculated mean strain and strain amplitude to show whether the device withstands 400 million cycles. In the plot the alternating strain value for diameter 23 mm is very close to the SN curve. Based on the haigh plot (Fig. 8) it was concluded that the device can with stand 400 million life cycles when deployed in the annulus diameter of 23 mm.

Radial force by compression testing: Based on the compression testing, the radial force was 14 N at 22 mm diameter (Fig. 10), almost similar to 16 N derived from FEA analysis. It is showing that the device has enough radial force below 22 mm diameter. The below plot is drawn by the taking the value from the compression testing machine which shows the radial force (N) vs. stent diameter (Fig. 9).

During TAVR, the stenotic aortic valve is balloon dilated and a biological valve sutured to the stent is implanted at the level of the aortic annulus. Once the native valve is ballooned and the transcatheter valve is deployed at the level of the aortic annulus, the device depends on radial expansive force of the nitinol stent to push the native valve aside and facilitate the anchorage of the tanscatheter valve to the annulus. In addition, transcatheter valve device depends on the radial force of the nitinol stent to create adequate seal between the device and the LVOT to prevent paraval vular leak. Based on the numeric modeling of the maximal blood pressure (230 mmHg), the minimal radial force required to prevent stent migration was 10 N.

One of the major advantages of the TAVR procedure is the ability to implant the valve through one of the peripheral arteries and avoid open-heart surgery. To achieve the ability to deploy the valve through a catheter driven through one of the peripheral arteries such as the femoral artery, valve-stent should be crimped to fit into a low profile delivery system (<24 F) and its material characterstics must not change. In the current study, 26 mm size nitinol stent prosthesis was modeled and the impact of varying design parameters on the radial force, crimp profile, buckling and fatigue were evaluated using FEA. The results indicate that for self-expanding nitinol stent, among various parameters, the height, thickness and number of struts of the rings influences both crimp diameter and the radial force. By optimizing thickness, height and number of struts of the nitinol stent it as possible to achieve optimal radial force of 14 N while attaining a crimp diameter of 3 mm. The optimized stent design showed adequate buckling strength and durability. Further mechanical testing will validate the final TAVR stent design.

Table 1: Fatigue anlysis strain table

Annuals diameter	Residual strain after deployment (%)	Strain for 150 mm of Hg (%) beam analysis	Strain for 50 mm of Hg (%) beam analysis	Actual strain for 50 mm of Hg (%)	Actual strain for 50 mm of Hg (%)
20	2.3	0.736	0.245	3.036	2.545
21	1.6	0.736	0.245	2.336	1.845
22	0.9	0.736	0.245	1.636	1.145
23	0.5	0.736	0.240	1.236	0.745

Table 2: Fatigue analysis-strain table

Annulus diameter	Residual strain after deployment strains (%)	Strain for 150 mm of Hg (Beam analysis)	Strain for 50 mm of Hg (Beam analysis)	Actual strain for 150 mm of Hg (%)	Actual strain for 50 mm of Hg (%)	Mean strain (%)	Alternating strains (%)
20	2.3	0.736	0.245	3.036	2.545	2.7905	0.2455
21	1.6	0.736	0.245	2.336	1.845	2.0905	0.2455
22	0.9	0.736	0.245	1.636	1.145	1.3905	0.2455
23	0.5	0.736	0.245	1.236	0.745	0.9905	0.2455

CONCLUSION

A unique Nitinol stent for TAVR was designed and analyzed using FEA. By optimizing various parameters, a Nitinol stent design with adequate radial force and low crimp diameter was achieved. Further in FEA, the stent design showed adequate buckling strength and durability. Based on the optimized stent design achieved by FEA, a composite Nitinol stent was prototyped. On mechanical testing, the prototype showed adequate radial force of 14 N, thus, confirming the results achieved by FEA. Further mechanical testing will validate the final stent design.

ACKNOWLEDGEMENT

This research work was supported by funding from Biotechnology Industry Research Assistance Council, Department of Biotechnology, Ministry of Science and Technology and Government of India-BT/BIPP0438/10/10.

REFERENCES

Booher, A.M. and K.A. Eagle, 2011. Diagnosis and management issues in thoracic aortic aneurysm. Am. Heart J., 162: 38-46.

Cunningham, P.M.S.M.E. and P.R.P.E. Barrett, 2004. Super elastic alloy eyeglass frame design using the ANSYS workbench environment. Ansys Computer Software Company, Canonsburg, Pennsylvania, USA. https://caeai.com/sites/default/files/Super_Elastic_Alloy_Eyeglass.pdf

Edwards, M.B. and K.M. Taylor, 2003. Outcomes in nonagenarians after heart valve replacement operation. Ann. Surg., 75: 830-834.

Ghanbari, H., A.G. Kidane, G. Burriesci, P. Bonhoeffer and A.M. Seifalian, 2008. Percutaneous heart valve replacement: An update. Trends Cardiovasc. Med., 18: 117-125.

Iung, B., G. Baron, E.G. Butchart, F. Delahaye and C. Gohlke-Barwolf *et al*., 2003. A prospective survey of patients with valvular heart disease in Europe: The euro heart survey on valvular heart disease. Eur. Heart J., 24: 1231-1243.

Jilaihawi, H., D. Chin, M. Vasa-Nicotera, M. Jeilan and T. Spyt *et al*., 2009. Predictors for permanent pacemaker requirement after transcatheter aortic valve implantation with the CoreValve bioprosthesis. Am. Heart J., 157: 860-866.

Kvidal, P., R. Bergstrom, L.G. Horte and E. Stahle, 2000. Observed and relative survival after aortic valve replacement. J. Am. Coll. Cardiol., 35: 747-756.

Lefèvre, T., A.P. Kappetein, E. Wolner, P. Nataf and M. Thomas *et al*., 2010. One year follow-up of the multi-centre European PARTNER transcatheter heart valve study. Eur. Heart J., 32: 148-157.

Lindroos, M., M. Kupari, J. Heikkilä and R. Tilvis, 1993. Prevalence of aortic valve abnormalities in the elderly: An echocardiographic study of a random population sample. J. Am. Coll. Cardiol., 21: 1220-1225.

Moat, N.E., P. Ludman, M.A. De-Belder, B. Bridgewater and A.D. Cunningham *et al*., 2011. Long-term outcomes after transcatheter aortic valve implantation in high-risk patients with severe aortic stenosis: The UK TAVI (United Kingdom transcatheter aortic valve implantation) registry. J. Am. Coll. Cardiol., 58: 2130-2138.

Otto, C.M., B.K. Lind, D.W. Kitzman, B.J. Gersh and D.S. Siscovick, 1999. Association of aortic-valve sclerosis with cardiovascular mortality and morbidity in the elderly. N. Eng. J. Med., 341: 142-147.

Passik, C.S., D.M. Ackermann, J.R. Pluth and W.D. Edwards, 1987. Temporal changes in the causes of aortic stenosis: A surgical pathologic study of 646 cases. Mayo Clin. Proc., 62: 119-123.

Roques, F., S.A. Nashef, P. Michel, E. Gauducheau and C. de Vincentiis *et al*., 1999. Risk factors and outcome in European cardiac surgery: Analysis of the EuroSCORE multinational database of 19030 patients. Eur. J. Cardiothorac. Surg., 15: 816-822.

Zahn, R., U. Gerckens, E. Grube, A. Linke and H. Sievert *et al*., 2010. Transcatheter aortic valve implantation: First results from a multi-centre real-world registry. Eur. Heart J., 32: 198-204.

Zajarias, A. and A.G. Cribier, 2009. Outcomes and safety of percutaneous aortic valve replacement. J. Am. Coll. Cardiol., 53: 1829-1836.